

Time Course of Gene Expression during *Porphyromonas gingivalis* Strain ATCC 33277 Biofilm Formation^{∇†}

Reiko Yamamoto, Yuichiro Noiri,* Mikiyo Yamaguchi, Yoko Asahi,
Hazuki Maezono, and Shigeyuki Ebisu

Department of Restorative Dentistry and Endodontology, Osaka University Graduate School of Dentistry,
1-8 Yamadaoka, Suita, Osaka 565-0871, Japan

Received 1 April 2011/Accepted 18 July 2011

Chronological gene expression patterns of biofilm-forming cells are important to understand bioactivity and pathogenicity of biofilms. For *Porphyromonas gingivalis* ATCC 33277 biofilm formation, the number of genes differentially regulated by more than 1.5-fold was highest during the growth stage (312/2,090 genes), and some pathogen-associated genes were time-dependently controlled.

Oral biofilms contain multiple bacterial species and cause opportunistic infections like dental caries and periodontal disease (3, 5). *Porphyromonas gingivalis*, a Gram-negative oral anaerobe, is distributed throughout oral biofilms and is one of the major pathogens in severe forms of marginal and refractory periapical periodontitis (14, 16). Global gene analysis using DNA microarray was performed on the planktonic cells of *P. gingivalis* ATCC 33277, and the total number of genes was reported to be 2,090 (11). Lo et al. (10) compared the global gene expression in a *P. gingivalis* strain W50 biofilm after 40 days of incubation with that of its planktonic counterparts grown in the same continuous culture relative to the gene expression data from strain W83. They found that in biofilm cells, genes involved in growth and metabolic activity were downregulated. However, time course gene expression changes during *P. gingivalis* biofilm formation have never been studied.

Biofilm formation is a dynamic and sequential process involving attachment, maturation, and detachment (17). It is important, therefore, to understand the changes in time course gene expression during biofilm growth. Recent microarray analyses of biofilms revealed that hundreds of genes, including many uncharacterized genes, are differentially expressed in biofilms; if fully characterized, they might provide insights into the genetic basis for biofilm formation (13). *P. gingivalis* biofilm 40 to 80 μm thick was formed on disks. A pump was used for 4 to 40 days to perfuse cell culture medium into the flow cell model (1, 4, 10, 15). Because it is possible to sequentially collect biofilm samples from initial adhesion to maturation, this model was chosen for the present study. The novel flow cell model is also valuable because of its high reproducibility and its ability to recover more biofilm-forming cells than the modified Robbins device (MRD) model (15).

The conditions used for the biofilm cell culture of *P. gingivalis* ATCC 33277 are described in the supplemental material. The biofilms were allowed to form for 14 days on hydroxyapatite (HA) powders using the flow cell model (see Fig. S1 in the supplemental material). The measurement of optical density at 550 nm (OD_{550}) and the confocal laser scanning microscopic (CLSM) observations were performed at 3, 6, 9 and 14 days. The OD_{550} value was lowest at day 3 and then increased sequentially to day 14 (Fig. 1). Individual *P. gingivalis* cells sparsely adhered to the disks at day 3 (Fig. 2A); between days 6 and 14, three-dimensional biofilm growth and a few red-stained dead cells were seen (Fig. 2B, C, and D). The volume of the biofilm was largest at day 14. Combining the images taken during biofilm growth (Fig. 2) with the OD values (Fig. 1) showed that the density of the biofilm-forming cells increased from days 3 to 6 and again from days 9 to 14 (Fig. 2).

The HA powders were rinsed and ultrasonicated for 30 min at 4°C in 20 ml of distilled water to release biofilm cells from the powders into the liquid. After isolation from the suspension of biofilm cells, the RNA was analyzed using the microarray (see supplemental material for details) and the gene expression data were normalized, generated, and assessed using a previously described method (see supplemental materials). The microarray data were deposited in the Center for Information Biology Gene Expression Database (CIBEX). The RNA samples harvested from the biofilm-forming cells after 3, 6, 9, and 14 days were named B1, B2, B3, and B4, respectively. The numbers of differentially expressed genes (DEGs) that were differentially regulated by more than 1.5-fold between each time point ($P < 0.01$, Welch t test) are shown in Fig. 3. The number of DEGs was highest between 9 days (B3) and 14 days (B4), when 155 genes were upregulated and 157 genes were downregulated. It is likely that the processes of biofilm maturation and of extracellular matrix formation are the processes that need changes in gene expression most.

The 52 genes that are known to be associated with the five virulence factors of *P. gingivalis* were selected, and the fold change data for each of them are shown in Table 1 (see also

* Corresponding author. Mailing address: Department of Restorative Dentistry and Endodontology, Osaka University Graduate School of Dentistry, 1-8 Yamadaoka, Suita, Osaka 565-0871, Japan. Phone and fax: 81-6879-2928. E-mail: noiri@dent.osaka-u.ac.jp.

† Supplemental material for this article may be found at <http://aem.asm.org/>.

∇ Published ahead of print on 29 July 2011.

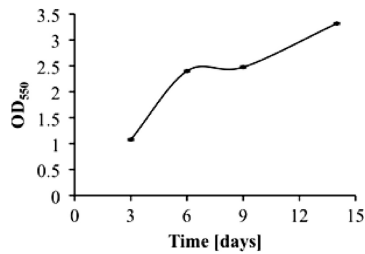


FIG. 1. *P. gingivalis* biofilm growth rate. Growth of *P. gingivalis* biofilm was analyzed quantitatively using the optical density method. The growth rate was not constant.

the supplemental material). Because the deletion of the gingipain-related genes *kgp* and/or *rgpA* *rgpB* promotes biofilm formation (6, 8), they might be predicted to be down-regulated during biofilm growth. However, in this study, the expression of gingipain-related genes was for the most part, constant; an exception was a subtle upregulation of PGN_0023 and *rgpB*, but this result was not significant ($P < 0.01$) (Table 1). An *rgpA* *rgpB* double mutant of *P. gingivalis* ATCC 33277 possessed very few fimbriae on the cell surface (7, 12). Although the deletion of both *rgpA* and *rgpB* had an impact on biofilm formation caused by defects in the fimbriae, the growth stage of the biofilm had no effect on the gene expression of the gingipain-related genes. During bio-

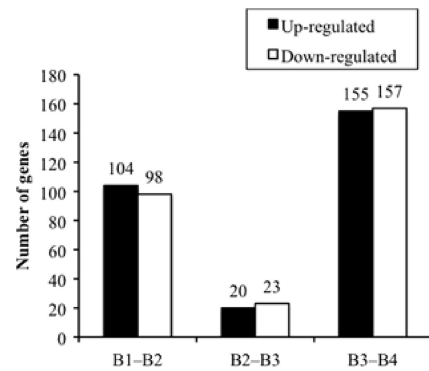


FIG. 3. Time-dependent changes for the numbers of differentially expressed genes of *P. gingivalis* biofilm-forming cells. The numbers of differentially expressed genes significantly upregulated (black bar) and downregulated (white bar) by more than 1.5-fold ($P < 0.001$, Welch t test) are shown.

film growth, *fimA* was upregulated between B1 and B2 and significantly downregulated in the following 3 days. A previous report found that the FimA fimbriae promoted initial biofilm formation but exerted a restraining regulation on biofilm maturation (8). These results suggested that in the early stage of biofilm formation the upregulation of *fimA* may encourage FimA fimbria production, thereby acceler-

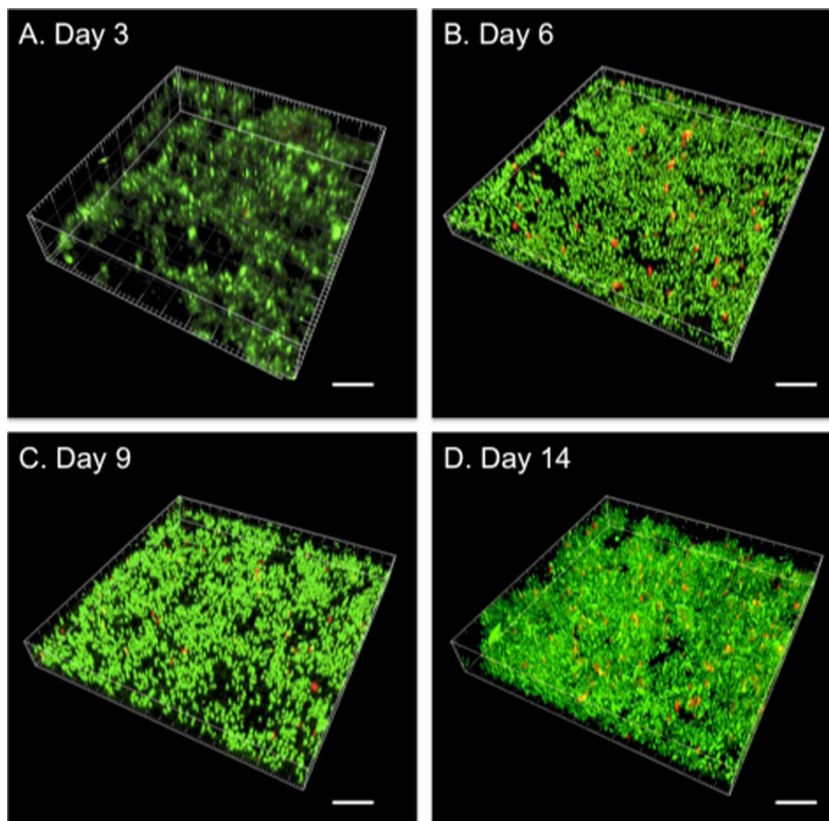


FIG. 2. CLSM images of *P. gingivalis* biofilm. *P. gingivalis* biofilm images at 3 (A), 6 (B), 9 (C), and 14 (D) days. Scale bar, 10 μ m. Live and dead cells are stained with green and red, respectively. The proportion of live to dead cells was $98.67\% \pm 0.10\%$ to $1.33\% \pm 0.10\%$ (A), $97.78\% \pm 0.40\%$ to $2.22\% \pm 0.40\%$ (B), $98.22\% \pm 0.17\%$ to $1.78\% \pm 0.17\%$ (C), and $98.75\% \pm 0.19\%$ to $1.25\% \pm 0.19\%$ (D).

TABLE 1. Fold change values for the differentially expressed genes associated with the virulence factors of *P. gingivalis*

Virulence factor	Locus tag	Fold changes ^a			Gene name	Product name ^b
		B1-B2 ^c	B2-B3 ^c	B3-B4 ^c		
Gingipain	PGN_0023	1.54	-1.68	1.56		Hypothetical protein
	PGN_0295	-1.32	1.41	1.05		C-terminal domain of Arg- and Lys-gingipainproteinase
	PGN_0778	-1.20	-1.24	1.45	<i>porT</i>	Membrane-associated protein PorT
	PGN_1466	1.52	-1.26	1.30*	<i>rgpB</i>	Arginine-specific cysteine proteinase RgpB
	PGN_1728	-1.12	1.09	1.03	<i>kgp</i>	Lysine-specific cysteine proteinase Kgp
	PGN_1768	1.25	-1.11	1.09		Putative DNA-binding response regulator/sensorhistidine kinase
	PGN_1970	1.08	-1.05	1.15	<i>rgpA</i>	Arginine-specific cysteine proteinase RgpA
	PGN_2065	1.14	-1.20	1.14		Putative Lys- and Rgp-gingipain domain protein
Hemagglutinin	PGN_0435	-1.24	1.03	1.27		Probable partial hemagglutinin-related protein
	PGN_0436	1.03	1.16	-1.20		Probable partial hemagglutinin-related protein
	PGN_0561	1.21	1.01	-1.03	<i>prtT</i>	Trypsinlike proteinase PrtT
	PGN_0900	1.00	1.20	1.02		Thiol protease
	PGN_1115	1.13	-1.08	1.02		Putative hemagglutinin
	PGN_1519	1.03	-1.18	1.17		Hemagglutinin-related protein
	PGN_1556	-1.24	1.06	-1.11		Putative hemagglutinin
	PGN_1733	-1.23*	-1.06	1.13	<i>hagA</i>	Hemagglutinin protein HagA
	PGN_1904	1.28	1.06	-1.21	<i>hagB</i>	Hemagglutinin protein HagB
	PGN_1906	1.28*	1.04	-1.17	<i>hagC</i>	Hemagglutinin protein HagC
PGN_2024	-1.11	-1.05	1.09		Putative hemagglutinin	
Fimbriae	PGN_0180	1.89*	-1.80*	1.39	<i>fimA</i>	FimA type I fimbilin
	PGN_0183	1.60*	-1.54*	1.03	<i>fimC</i>	Minor component FimC
	PGN_0184	-1.20	1.01	1.40	<i>fimD</i>	Minor component FimD
	PGN_0185	-1.38*	1.11	1.36	<i>fimE</i>	Minor component FimE
	PGN_0287	1.62*	-1.21	1.13	<i>mfaI</i>	MfaI fimbilin
	PGN_0288	1.68*	-1.13	-1.22*		Hypothetical protein
LPS	PGN_0206	1.26	-1.33	1.47*		Putative lipid A disaccharide synthase
	PGN_0376	1.00	-1.06	1.33*		2-Dehydro-3-deoxyphosphooctonate aldolase
	PGN_0524	-1.21	1.21	-1.09		Hypothetical protein
	PGN_0544	1.07	-1.14	1.43*		3-Deoxy-D-manno-octulosonic acid transferase
	PGN_0679	1.42	-1.32	-1.08		Putative tetraacyldisaccharide 4'kinase
	PGN_0696	1.10	-1.03	1.28*		Probable hydrolase
	PGN_0777	1.27	-1.57*	1.32		Probable glycosyl transferase
	PGN_1054	-1.20	-1.08	1.82*	<i>vimF</i>	Virulence-modulating gene F
	PGN_1134	-1.08	-1.10	1.38		Hypothetical protein
	PGN_1235	-2.19*	1.83*	-1.37	<i>porS</i>	Membrane protein PorS
	PGN_1239	-1.51	1.10	-1.10		Probable lipopolysaccharide biosynthesisglycosyltransferase
	PGN_1240	-1.12	1.37	-1.24		Hypothetical protein
	PGN_1251	-1.48	1.28	1.03		Probable glycosyltransferase
	PGN_1255	1.04	1.28	-2.64*		Putative heptosyltransferase
	PGN_1302	-1.25	1.29	1.16		Hypothetical protein
	PGN_1310	-2.84	1.64	-1.73*		Glycogen synthase
	PGN_1481	-1.17	1.08	1.33		Putative polysaccharide biosynthesis protein
	PGN_1614	-1.53*	1.31	-1.72*		UDP-glucose 4-epimerase
	PGN_1713	-1.09	-1.09	1.43		Hypothetical protein
	PGN_1718	1.03	1.16	-2.09*		Probable UDP-2,3-diacetylglucosamine hydrolase
	PGN_1736	-1.28	1.12	-1.03		Putative glycogen synthase
	PGN_1750	1.59	-1.25	-1.36*		Putative 3-deoxy-D-manno-octulosonatecytidyltransferase
	PGN_2018	3.45	-1.37	-2.74*		Putative UDP-N-acetylglucosamineacetyltransferase
PGN_2019	2.64*	-1.19	-2.32*		UDP-3-O-[3-hydroxymyristoyl] N-acetylglucosamine deacetylase	
PGN_2020	1.37	-1.11	-1.60*		UDP-3-O-[3-hydroxymyristoyl] glucosamine N-acyltransferase	
PGN_2086	-1.07	1.00	1.23		Probable acetyltransferase	
Capsule	PGN_1100	-1.15	1.22*	-1.29*		Putative capsule biosynthesis protein CapA

^a Bold text indicates a fold change of more than 1.5 or less than -1.5. *, *P* < 0.001 for the Welch *t* test. Shaded text indicates that the changes satisfy two criteria: a fold change of more than 1.5 or less than -1.5 and a statistically significant difference (*P* < 0.01, Welch *t* test).
^b The product name is from the *P. gingivalis* ATCC 33277 genome database (http://www.ncbi.nlm.nih.gov/sites/entrez?Db=genome&Cmd=Retrieve&dopt=Protein+Table&list_uids=22372).
^c B1, B2, B3, and B4 refer to the RNA samples harvested from the biofilm-forming cells after 3, 6, 9, and 14 days, respectively.

ating the attachment of the cells to the surface; suppression of *fimA*, on the other hand, may function as a switch for biofilm maturation. Deletion of *clpXP*, one of the members of the heat shock protein family, caused overexpression of *mfa1* and accelerated biofilm formation (2), and while the wild-type strain formed microcolonies, an *mfa1* mutant did not (9). Our results are consistent with those of the earlier studies and support the speculation that *mfa1* acts from the B1 stage to the B2 stage. Lipopolysaccharide (LPS)-related PGN_2019 was significantly upregulated between B1 and B2, and seven genes were significantly downregulated between B3 and B4. It is likely that, at the later stages of biofilm formation, the downregulation of the fimbria- and LPS-related genes might be associated with the detachment of cells.

In conclusion, many genes were found to be time-dependently regulated during *P. gingivalis* ATCC 33277 biofilm growth, suggesting that they may be related to the pathogenicity of *P. gingivalis*.

Database sequence accession number. The entire set of microarray data has been deposited in the Center for Information Biology Gene Expression Database (CIBEX) (<http://cibex.nig.ac.jp/index.jsp>) under accession number CBX149.

This study was supported by Grants-in-Aid for Scientific Research (20249076 and 21390508) by the Japan Society for the Promotion of Science.

REFERENCES

1. Asahi, Y., et al. 2010. Effects of N-acyl homoserine lactone analogues on *Porphyromonas gingivalis* biofilm formation. *J. Periodontol. Res.* **45**:255–261.
2. Capestany, C. A., G. D. Tribble, K. Maeda, D. R. Demuth, and R. J. Lamont. 2008. Role of the Clp system in stress tolerance, biofilm formation, and intracellular invasion in *Porphyromonas gingivalis*. *J. Bacteriol.* **190**:1436–1446.
3. Costerton, J. W., P. S. Stewart, and E. P. Greenberg. 1999. Bacterial biofilms: a common cause of persistent infections. *Science* **284**:1318–1322.
4. Davey, M. E. 2006. Techniques for the growth of *Porphyromonas gingivalis* biofilms. *Periodontol.* **2000** **42**:27–35.
5. Donlan, R. M., and J. W. Costerton. 2002. Biofilms: survival mechanisms of clinically relevant microorganisms. *Clin. Microbiol. Rev.* **15**:167–193.
6. Grenier, D., et al. 2003. Effect of inactivation of the Arg- and/or Lys-gingipain gene on selected virulence and physiological properties of *Porphyromonas gingivalis*. *Infect. Immun.* **71**:4742–4748.
7. Kadowaki, T., et al. 1998. Arg-gingipain acts as a major processing enzyme for various cell surface proteins in *Porphyromonas gingivalis*. *J. Biol. Chem.* **273**:29072–29076.
8. Kuboniwa, M., et al. 2009. Distinct roles of long/short fimbriae and gingipains in homotypic biofilm development by *Porphyromonas gingivalis*. *BMC Microbiol.* **9**:105.
9. Lin, X., J. Wu, and H. Xie. 2006. *Porphyromonas gingivalis* minor fimbriae are required for cell-cell interactions. *Infect. Immun.* **74**:6011–6015.
10. Lo, A. W., et al. 2009. Comparative transcriptomic analysis of *Porphyromonas gingivalis* biofilm and planktonic cells. *BMC Microbiol.* **9**:18.
11. Naito, M., et al. 2008. Determination of the genome sequence of *Porphyromonas gingivalis* strain ATCC 33277 and genomic comparison with strain W83 revealed extensive genome rearrangements in *P. gingivalis*. *DNA Res.* **15**:215–225.
12. Nakayama, K., F. Yoshimura, T. Kadowaki, and K. Yamamoto. 1996. Involvement of arginine-specific cysteine proteinase (Arg-gingipain) in fimbriation of *Porphyromonas gingivalis*. *J. Bacteriol.* **178**:2818–2824.
13. Niba, E. T., Y. Naka, M. Nagase, H. Mori, and M. Kitakawa. 2007. A genome-wide approach to identify the genes involved in biofilm formation in *E. coli*. *DNA Res.* **14**:237–246.
14. Noguchi, N., Y. Noiri, M. Narimatsu, and S. Ebisu. 2005. Identification and localization of extraradicular biofilm-forming bacteria associated with refractory endodontic pathogens. *Appl. Environ. Microbiol.* **71**:8738–8743.
15. Noiri, Y., et al. 2003. Effects of chlorhexidine, minocycline, and metronidazole on *Porphyromonas gingivalis* strain 381 in biofilms. *J. Periodontol.* **74**:1647–1651.
16. Noiri, Y., L. Li, F. Yoshimura, and S. Ebisu. 2004. Localization of *Porphyromonas gingivalis*-carrying fimbriae in situ in human periodontal pockets. *J. Dent. Res.* **83**:941–945.
17. Sauer, K., A. K. Camper, G. D. Ehrlich, J. W. Costerton, and D. G. Davies. 2002. *Pseudomonas aeruginosa* displays multiple phenotypes during development as a biofilm. *J. Bacteriol.* **184**:1140–1154.